JCTC Journal of Chemical Theory and Computation

Article

pubs.acs.org/JCTC

Components of the Bond Energy in Polar Diatomic Molecules, Radicals, and Ions Formed by Group-1 and Group-2 Metal Atoms

Haoyu Yu and Donald G. Truhlar*

Department of Chemistry, Chemical Theory Center, and Supercomputing Institute, University of Minnesota, Minneapolis, Minnesota 55455-0431, United States

Supporting Information

ABSTRACT: Although many transition metal complexes are known to have high multireference character, the multireference character of main-group closed-shell singlet diatomic molecules like BeF, CaO, and MgO has been less studied. However, many group-1 and group-2 diatomic molecules do have multireference character, and they provide informative systems for studying multireference character because they are simpler than transition metal compounds. The goal of the present work is to understand these multireference systems better so that, ultimately, we can apply what we learn to more complicated multireference systems and to the design of new exchange-correlation functionals for treating multireference systems more adequately. Fourteen main-group diatomic molecules and one triatomic molecule (including radicals, cations, and anions, as well as neutral closed-shell species) have been studied for this article. Eight of these molecules contain a group-1 element, and six contain a group-2 element. Seven of these molecules are multireference systems, and eight of them are single-reference systems. Fifty-three exchange-correlation functionals of 11 types [local spin-density approximation (LSDA), generalized gradient approximation (GGA), nonseparable gradient approximation (NGA), global-hybrid GGA, meta-GGA, meta-NGA, global-hybrid meta GGA, range-separated hybrid GGA, range-separated hybrid meta-GGA, range-separated hybrid meta-NGA, and DFT augmented with molecular mechanics damped dispersion (DFT-D)] and the Hartree−Fock method have been applied to calculate the bond distance, bond dissociation energy (BDE), and dipole moment of these molecules. All of the calculations are converged to a stable solution by allowing the symmetry of the Slater determinant to be broken. A reliable functional should not only predict an accurate BDE but also predict accurate components of the BDE, so each bond dissociation energy has been decomposed into ionization potential (IP) of the electropositive element, electron affinity of the electronegative bonding partner (EA), atomic excitation energy (EE) to prepare the valence states of the interacting partners, and interaction energy (IE) of the valence-prepared states. Adding Hartree−Fock exchange helps to obtain better results for atomic excitation energy, and this leads to improvements in getting the right answer for the right reason. The following functionals are singled out for reasonably good performance on all three of bond distance, BDE, and dipole moment: B97-1, B97-3, MPW1B95, M05, M06, M06-2X, M08-SO, N12-SX, O3LYP, TPSS, τ-HCTHhyb, and GAM; all but two (TPSS and GAM) of these functionals are hybrid functionals.

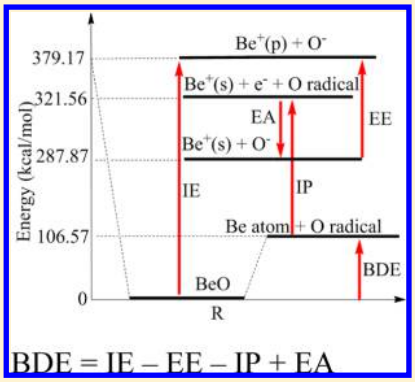

1. INTRODUCTION

Multireference systems are systems for which accurate wave function calculations require a multiconfigurational reference state because the system is inherently multiconfigurational. These systems are also called strongly correlated. With the exact exchange-correlation functional, Kohn−Sham density functional theory (KS DFT) is exact for both single-reference and multireference systems, even though the density is represented by a single Slater determinant. However, the exact functional is unknown and probably unknowable, and with currently available functionals, KS DFT is more accurate for single-reference systems than for multireference ones.

Transition metals and their complexes are well-known to often have multireference character because many interesting systems (for example, bare atoms and molecules with less than eighteen valence electrons) have unfilled valence-shell orbitals, and the near degeneracies of the s and d electrons can lead to multiple low-energy electron configurations. However, main-group diatomic molecules can also have multireference character, and their electronic structure is, in principle, easier to understand. So, they provide a testing ground for theory that lies between main-group nonmetallic chemistry and transition metal chemistry. Understanding main-group diatomic molecules is, therefore, a useful complement to direct study of transition metal systems, as well as being of interest in its own right. Main-group molecules are usually easier to study than transition metals not only because their atoms do not have incomplete d subshells but also because they may have fewer electrons than typical transition metal compounds.

Diatomic molecules contain only one chemical bond, and we can draw more unambiguous conclusions about their treatment

Received: January 29, 2015
Published: May 26, 2015

DOI: 10.1021/acs.jctc.5b00083
J. Chem. Theory Comput. 2015, 11, 2968−2983

than we can for polyatomic molecules. For this reason, and because Ca is the main-group metal most similar to a 3d transition metal, in a very recent article, we studied the CaO molecule in detail.[1] In our study of CaO, not only did we study the bond dissociation energy but also we partitioned the bond dissociation energy into physical components. We did this by envisioning the bond forming process to occur in several steps, as follows

(1) Ca is ionized by losing an electron; the energetic cost is the ionization potential (IP) of Ca.
(2) O attaches the electron; this process releases energy equal to the electron affinity (EA).
(3) $Ca^+(s)$ is excited to $Ca^+(d)$, which is its valence state, i.e., a description of the orbital occupancy that it has after the bond is formed; the cost for this is the corresponding excitation energy (EE) of Ca^+. Now, the partners are both in their valence states and ready to interact.
(4) The interaction of $Ca^+(d)$ and O^- releases energy; this is called the interaction energy between two prepared states (IE).

A theory that predicts the correct bond dissociation energy (BDE) for the right reason, rather than by cancellation of errors, should not only predict an accurate value for the BDE but also predict correct values for these four components. We will use the same strategy to ascertain the reliability of exchange-correlation functionals for 15 molecules in the present article, and this broader test set should allow us to draw more robust conclusions.

In order to fully understand why exchange-correlation functionals often fail for multireference systems, we will study the BDE and dipole moments of 14 diatomic molecules and one triatomic molecule in this article. Fourteen of the molecules contain a main-group metal, and we also include the HF molecule for comparison. In particular, in the present article, we study BeF radical, BeO, BeO^+ radical cation, HF, KF, KO^-, KOH, LiF, LiO radical, LiO^-, MgO, MgS, NaO radical, and NaO^-, and we will include the previously studied CaO in our 15-molecule test set. Some of these 15 molecules have been studied by Martin using the W4 method.[2,3] The heats of formation and structures of BeO, MgO, KOH, and CaO have been studied with CCSD(T),[4] B3LYP,[5] and MP2 methods.[6,7] Martin concluded that core-correlation should be included, which requires additional basis functions as compared to the usual basis sets that are extended only for valence electrons, and that the molecules BeO, MgO, and CaO have multireference character that provides a challenge for high-level ab initio methods.[8] Some other studies of various chemical properties of BeO have also been reported, for example, the valence band gap of BeO has been studied by Soulé de Bas et al.,[9] the valence states of BeO have been study by Sorensen et al.,[10] and the low-lying states of BeO have been studied by Irisawa et al.[11] The partial atomic charges and dipole moment of LiF, KF, BeO, and MgO have been studied by Nakazato et al.[12] In the present article, we will study the BDE, IP, EA, EE, IE, and dipole moments for 14 main-group diatomic molecules and one triatomic molecule (KOH).

2. COMPUTATIONAL DETAILS

The geometries that we used to calculate various diagnostics are obtained by employing the M06[13] exchange-correlation functional with the ma-TZVP basis set.[14] Bond dissociation energy, ionization potential, electron affinity, atomic excitation energy, interaction energy between two prepared states, and dipole moments are calculated with the cc-pCVQZ[15] basis set for all metal atoms, the aug-cc-pCVQZ basis set[16] for oxygen, fluorine, and sulfur, and the cc-pVQZ basis set for hydrogen. The geometries used to calculate bond dissociation energy and dipole moment are optimized with each individual method. We did stability tests[17,18] on all of the molecular and atomic systems involved in this study by using the stable=opt keyword of *Gaussian 09*.[19] This keyword allows the program to test all instabilities of the wave function and then search for a lower energy.

Dipole moments of charged molecules depend on the origin, and for the present article, we take that as the center of nuclear charge.

CASSCF[20] calculations with full valence space are used to calculate the M diagnostic.[21] All benchmark values are from experiments and high-level calculations. In this article, we use CCSDT/aug-cc-pCVQZ method[16,22] and CCSDT(Q)2/aug-cc-pCVQZ method[16,22] in *NWChem*[23] to obtain some of the benchmark values. T_1,[24] TAE(T),[2] and B_1[21,25,26] diagnostics were calculated using *Gaussian 09*;[19] M diagnostic[21] was calculated using *Molpro*.[27]

3. RESULTS AND DISCUSSION

3.1. Multireference Character. In order to categorize the electronic structure of the molecules, we applied four diagnostics to these molecules, in particular, the T_1, TAE(T), M, and B_1 diagnostics. We explained all four diagnostics in detail in our previous paper,[1] but we will review them briefly in the following paragraphs. The first three are multireference diagnostics; B_1 is a broader diagnostic that might better be viewed as a difficult case diagnostic, although here we use it as a multireference diagnostic. The results for all of the diagnostics are listed in Table 1.

Lee and Taylor proposed the T_1 diagnostic in 1989; it is the norm of the vector of single-excitation amplitudes in a closed-shell coupled-cluster singles and doubles wave function.[24] For the T_1 diagnostic, if T_1 is smaller than 0.02, then the system under consideration is considered to be a single-reference system; if T_1 is equal or larger than 0.02, then the system under consideration is a multireference system.[23]

TAE[T] is defined as[2]

$$\%\ \mathrm{TAE[T]} = 100\left(\frac{\mathrm{AE[CCSD(T)]} - \mathrm{AE[CCSD]}}{\mathrm{AE[CCSD(T)]}}\right) \quad (1)$$

where AE[CCSD(T)] is the atomization energy calculated with the CCSD(T) method[4] and AE[CCSD] is the atomization energy calculated with the CCSD method.[28−31] If TAE(T) is smaller than 2%, then the system under consideration is classified as a single-reference system; if TAE(T) is equal to or larger than 2%, then the system under consideration is classified as a multireference system.[2]

The B_1 diagnostic is defined for a single bond as

$$B_1 = [D_e(\mathrm{BLYP}) - D_e(\mathrm{B1LYP//BLYP})] \quad (2)$$

where D_e(BLYP) is the bond dissociation energy of a molecule calculated by the BLYP[32,33] exchange-correlation functional and B1LYP//BLYP stands for a B1LYP[34] calculation with the geometries of the molecule and the fragments optimized by the BLYP exchange-correlation functional. For the B_1 diagnostic, if B_1 is smaller than 10.0 kcal/mol per chemical bond, then the system under consideration is diagnosed as a single-reference system; if B_1 is equal to or larger than 10.0 kcal/mol per chemical bond, then the system under consideration is diagnosed as a multireference system.[21,25,26]

DOI: 10.1021/acs.jctc.5b00083
J. Chem. Theory Comput. 2015, 11, 2968−2983

Table 1. Multireference Diagnostics and CM5 Charges on the Metal Atoms[a,b]

	T_1 diagnostic	TAE(T) diagnostic	B_1 diagnostic (kcal/mol)	M diagnostic	MR[a]	q_M
BeF radical	0.015	0.021	5.5	0.019	0	0.46
BeO	0.042	0.078	14.9	0.043	4	0.81
BeO^+	0.019	0.029	6.4	0.032	0	1.31
CaO	0.037	0.117	21.7	0.043	4	0.85
HF	0.0098	0.013	5.0	0.020	0	0.26
KF	0.016	0.021	2.1	0.0092	0	0.77
KO^-	0.066	0.42	20.9	0.84	4	0.01
KOH	0.015	0.031	5.2	0.023	0	0.81
LiF	0.015	0.017	6.6	0.021	0	0.69
LiO radical	0.015	0.024	5.8	0.031	0	0.65
LiO^-	0.10	0.17	15.5	0.053	4	0.01
MgO	0.053	0.24	19.2	0.16	4	0.74
MgS	0.029	0.14	6.3	0.16	3	0.63
NaO radical	0.020	0.038	6.0	0.031	0	0.68
NaO^-	0.064	0.29	19.9	0.70	4	−0.02

[a]The number in the MR column indicates how many diagnostics out of four indicate that the molecule is a multireference system. [b]The charge on the metal atom (or H in HF) is computed by Charge Model 5 (CM5) using the MPWLYP1 M exchange-correlation functional and the ma-TZVP basis set.

The M diagnostic for a closed-shell singlet is defined as

$$M = \frac{1}{2}(2 - n(\mathrm{MCDONO}) + n(\mathrm{MCUNO})) \quad (3)$$

The M diagnostic for an open-shell system is defined as

$$M = \frac{1}{2}(2 - n(\mathrm{MCDONO}) + \sum_{j=1}^{n_{\mathrm{SOMO}}} |n(j) - 1| + n(\mathrm{MCUNO})) \quad (4)$$

In eqs 3 and 4, n is the natural orbital occupation number, MCDONO stands for the most correlated doubly occupied natural orbital, and MCUNO stands for the most correlating unoccupied natural orbital. In eq 4, n_{SOMO} stands for the number of singly occupied natural orbitals. If M is smaller than 0.04, then the system under consideration is considered to be a single-reference system; if M is equal to or larger than 0.04, then the system under consideration is considered to be a multireference system.[21]

The four diagnostics agree with each other except for MgS. Only the B_1 diagnostic indicates that MgS is a single-reference system; the others imply that MgS is a multireference system. On the basis of the three or more diagnostics telling us that a molecule has multireference character, the results in Table 1 show that seven of the molecules studied here have multi-reference character, even though the elements that they contain are all from the main group. In particular, BeO, CaO, KO^-, LiO^-, MgO, MgS, and NaO^- are multireference systems, and the BeF radical, BeO^+, HF, KF, KOH, LiF, LiO radical, and NaO radical are single-reference (SR) systems.

Main-group molecules are usually easier to study than transition metals. First, main-group molecules may have fewer electrons than typical transition metal compounds. Second, the diatomic molecules we studied in this article contain only one chemical bond. In order to fully understand why exchange-correlation functionals fail for multireference systems, we will study BDE and dipole moments of these 14 diatomic molecules and one triatomic molecule in this article. Fourteen of the molecules contain a main-group metal, and we also include the HF molecule for comparison.

3.2. Ionic Character. Table 1 also shows the CM5 charges[35] of the metal atoms (or hydrogen in the case of HF) of the 15 molecules under consideration. The molecules that are mainly dominated by ionic bonds are BeO, CaO, KF, KOH, LiF, LiO, MgO, MgS, and NaO, with charges on the metal atoms of more than 0.5. The molecules that are mainly dominated by nonpolar covalent bonds are LiO^-, KO^-, and NaO^-, with the CM5 charge on the metal atoms less than 0.02. The molecules that are formed by polar covalent bonds are BeF, BeO^+, and HF; for these, the CM5 charge on the more electropositive element is 0.46, 1.31, and 0.26, respectively.

3.3. Bond Energies. We applied 53 exchange-correlation functionals and Hartree−Fock theory to calculate the energies of all 15 molecules and their lowest-energy dissociation products. We added PW6B95-D3(0) and PW6B95-D3(BJ) to the 49 functionals tested in our previous paper[1] because of the good performance against the GMTKN30 database tested by Grimme.[36] We also added two functionals, namely, GAM[37] and revB3LYP.[38] GAM is a new functional published by our group, and revB3LYP was suggested by the reviewers. We list all of the methods in Table 2 with the percentage of Hartree−Fock exchange, the type of functional, and the original reference.

Bond dissociation energies are evaluated by 54 methods including 53 exchange-correlation functionals and the Hartree−Fock method. The benchmark values of the bond dissociation energies of the 15 molecules come from experiment and high-level calculations. Table 3 shows all of the benchmark values of all 15 molecules. For bond dissociation energy, we first obtain the D_0 from the reference and then add zero point energy to D_0 to get D_e; we also provide the experimental ionization potential (IP), electron affinity (EA), atomic excitation energy (EE), interaction energy between two prepared states (IE), and dipole moments for 15 molecules in Table 3. All calculations in the present article are nonrelativistic. We do check the scalar relativistic effect by the second order Douglas−Kroll−Hess[39−41] and spin−orbit correction for all 15 main-group molecules in Table 3. Spin−orbit corrections of all atoms, cations, and anions are from ref 42, and the others are calculated at the CASSCF/ma-TZVP level of theory using *Molpro*.[43] The average percentage of total relativistic effect is 1.75% of the average BDE of 15 diatomic

DOI: 10.1021/acs.jctc.5b00083
J. Chem. Theory Comput. 2015, 11, 2968−2983

Table 2. Exchange-Correlation Functionals Tested in This Article

type	method	ref	X^a
LSDA	GVWN5[b]	55−57	0
GGA	BB95	32, 58	0
	BLYP	32, 33	0
	MOHLYP	25	0
	OHLYP	33, 59	0
	OLYP	33, 59	0
	OreLYP	33, 59, 60	0
	PBE	61	0
	SOGGA	62	0
	SOGGA11	63	0
NGA	N12	64	0
	GAM	37	0
meta-GGA	M06-L	65	0
	M11-L	66	0
	revTPSS	67	0
	TPSS	68	0
meta-NGA	MN12-L	69	0
global hybrid GGA	B1B95	58	25
	B1LYP	34	25
	B3LYP	5	20
	B3LYP*	70	15
	revB3LYP	38	20
	B97-1	71	21
	B97-3	72	26.93
	HFLYP	73	100
	MPW1K	74	42.8
	MPWLYP1M	25	5
	O3LYP	75	11.61
	PBE0	76	25
	SOGGA11-X	77	35.42
global hybrid meta-GGA	BB1K	78	42
	M05	79	28
	M05-2X	80	56
	M06	13	27
	M06-2X	13	54
	M08-HX	81	52.23
	M08-SO	81	56.79
	MPW1B95	82	31
	MPWB1K	82	44
	PW6B95	83	28
	revTPSSh	84	10
	TPSSh	85	10
	τ-HCTHhyb	86	15
range separated hybrid GGA	CAM-B3LYP	87	19−65
	HSE06	88, 89	0−25
	ωB97	90	100
	ωB97X	90	15.77−100
range separated hybrid NGA	N12-SX	91	5−60
range separated hybrid meta-GGA	M11	92	42.8−100
range separated hybrid meta-NGA	MN12-SX	91	25−0
DFT-D	ωB97X-D	93	22.2−100
	PW6B95-D3(0)	36	28
	PW6B95-D3(BJ)	94−96	28

[a] X is the percentage of nonlocal Hartree−Fock exchange. When a range is given, the first value is for small interelectronic distances, and the second value is used for large interelectronic distances. Details of the functional forms that join these regions of interelectronic separation are given in the references. [b] GVWN5 denotes the Gáspár approximation for exchange and the VWN5 fit to the correlation energy; this is an example of the local spin density approximation (LSDA), and it has the keyword SVWN5 in the *Gaussian 09* program. Note that Kohn−Sham exchange is the same as Gáspár exchange, but Slater exchange (not tested here) is higher by a factor of 1.5.

molecules. This small correction will not affect the conclusions of our article. Therefore, we do not include relativistic effect in the rest of our calculations. We obtain some of the benchmark values from couple-cluster calculations. For BeO^+, KO^-, LiO^-, and NaO^-, we obtain the D_e from CCSDT(Q)2 and CCSD(T) calculations. For BeF, BeO, BeO^+, CaO, KO^-, LiO^-, MgS, NaO, and NaO^-, we obtain the dipole moment from CCSDT calculations. We also show the experimental equilibrium bond distances (R_e) for 12 molecules (BeF, BeO, BeO+, CaO, HF, KF, KOH, LiF, LiO, MgO, MgS, and NaO) in Table 3.

We present both mean unsigned errors (MUEs) and mean signed errors (MSEs) of the BDE in Table 4 for all of the molecules in our database. The MUEs show that the best functional for the 15 main-group molecules is M08-HX, which gives a MUE of 3.77 kcal/mol, and the second best is ωB97X-D, with a MUE of 3.82 kcal/mol; the third best is TPSS, with a MUE of 3.92 kcal/mol. The fourth best is PW6B95-D3(BJ) with a MUE of 3.94 kcal/mol. By adding damped dispersion corrections to the PW6B95 density functional, the MUE is reduced from 4.00 to 3.94 and 3.97 kcal/mol for PW6B95-D3(BJ) and PW6B95-D3(0), respectively. As a result, two of the top four most accurate density functionals for the MUE of the BDE have empirical molecular mechanics terms. Of the other six functionals in the top eight, three (TPSS, OreLYP, and revTPSS) have no Hartree−Fock exchange. In the last column of Table 4, we show the MSE of each function in predicting the BDE; the MSE shows whether there are systematic errors (whether the average bond energies are being overestimated (positive) or underestimated (negative)). Some functionals, for example, N12, B3LYP, and CAM-B3LYP, have a small MSE but a much larger MUE.

In order to understand the multireference character of these molecules, we divide them into two groups: one group consists of eight single-reference molecules, and the other group consists of seven multireference molecules. In Table 4, we show the MUEs and MSEs for single-reference molecules and multireference molecules in the MR and SR columns, respectively. We find that M08-HX, GAM, M08-SO, revTPSS, SOGGA11-X, PW6B95, PW6B95-D3(0), PW6B95-D3(BJ), M06-2X, and B97-3 predict the BDE of single-reference molecules very well; MOHLYP, B1LYP, TPSS, τ-HCTHhyb, M08-HX, HSE06, PW6B95, PW6B95-D3(0), PW6B95-D3(BJ), and OreLYP predict the BDE of multireference molecules well; M08-HX, PW6B95-D3(0), PW6B95-D3(BJ), PW6B95, OreLYP, revTPSS, and ωB97X-D are in both groups and therefore predict both single-reference molecules and multireference molecules well (they are within the top 12 in predicting the BDE of single-reference and multireference systems). In order to understand the source of the errors in the BDE, we break the BDE into several parts according to how the bond of each molecule is formed.

DOI: 10.1021/acs.jctc.5b00083
J. Chem. Theory Comput. 2015, 11, 2968−2983

Table 3. Benchmark Values of Equilibrium Bond Distance, Bond Dissociation Energy, Ionization Potential, Electron affinity, Atomic Excitation Energy, Interaction Energy between Two Prepared States, and Dipole Moment for All 15 Main-Group Molecules[a]

	R_e[m]	D_0[c]	ω[f]	D_e[b]	IP[d]	EA[e]	EE[g]	IE[h]	DM[i]	SO[j]	SR[k]	total relativistic effects[l]
BeF	1.361	136.95	1247.36	138.73	214.99	78.43		275.29	1.18	0.01	−2.50	−2.49
BeO	1.331	104.44	1487.32	106.57	214.99	33.69	91.30	379.17	6.21	−0.22	−0.27	−0.49
BeO^+	1.43			84.42	419.97	33.69		470.70	7.25	−0.06	0.16	0.10
CaO	1.821	95.10	732.03	96.15	140.97	33.69	39.10	242.53	8.73	−0.22	−1.22	−1.44
HF	0.917	136.15	4138.39	142.07	313.59	78.43		377.23	1.83	−0.38	−0.68	−1.06
KF	2.171	116.92	426.26	117.53	100.10	78.43		139.20	8.59	−0.38	−0.44	−0.82
KO^-				33.14					2.16	−0.16	−1.16	−1.32
KOH	2.212, 0.91			85.00	100.10	42.15		142.95	7.42	−0.20	1.33	1.13
LiF	1.564	137.90	910.57	139.20	124.34	78.43		185.11	6.33	−0.38	−0.55	−0.93
LiO	1.688	81.38	814.62	82.54	124.34	33.69		173.19	6.84	−0.06	0.14	0.08
LiO^-				57.59			42.61	100.20	3.06	−0.16	0.71	0.55
MgO	1.749	61.11	785.21	62.23	176.33	33.69		204.87	6.20	−0.22	2.52	2.30
MgS	2.143	55.93	528.74	56.68	176.33	47.90		185.11	7.31	−0.56	−1.26	−1.82
NaO	2.052	64.53	492.30	65.24	118.51	33.69		150.06	8.26	−0.22	−1.43	−1.65
NaO^-				39.55					0.51	−0.16	−1.62	−1.78

[a] D_0, D_e, ionization potential (IP), electron affinity (EA), excitation energy (EE), interaction energy between two prepared states (IE), spin−orbit correction (SO), scalar relativistic effects (SR), and total relativistic effects have units of kcal/mol; bond distance (R_e) has the unit of Å, ω has units of cm^{-1}, and dipole moment has units of debye. [b] D_e is the equilibrium bond dissociation energy: $D_e = D_0$ + ZPE, where ZPE is the zero point energy. [c] The benchmark values of D_0 for BeF, BeO, BeO^+, CaO, HF, KF, KOH, LiF, LiO, MgS, and NaO are taken from ref 45. The benchmark values of D_0 for KO^-, LiO^-, and NaO^- are calculated by the CCSDT method. The benchmark value of D_0 for MgO is taken from ref 46. [d] The benchmark values of IP are from ref 47. [e] The benchmark values of EA for F, O, and S are from ref 48. The benchmark value of EA for OH is from ref 49. [f] The benchmark values of spectroscopic constants ω are from ref 50. [g] The benchmark values of EE for Ca^+, Be^+, and Li are from ref 42. [h] The benchmark values of IE are calculated by using the following equation: IE = BDE + IP + EE − EA [i] DM denotes dipole moment. The benchmark values of DM for HF, LiF, LiO, and MgO are from ref 35. The benchmark value of DM for KF is from ref 51. The benchmark values of DM for the remaining 11 molecules are calculated with the CCSDT method. [j] The spin−orbit corrections for F, O, S, and O^- are from ref 42. The spin−orbit correction for BeF, BeO^+, and LiO are calculated at the CASSCF/ma-TZVP level of theory using *Molpro*. [k] The scalar relativistic effects are calculated by the second-order Douglas−Kroll−Hess method in *Gaussian 09*. [l] The total relativistic effect is the summation of spin−orbit correction and the scalar relativistic effect. [m] The experimental equilibrium bond distances of 12 molecules are given in the second column. The experimental bond distances for BeF, BeO, HF, KF, LiF, LiO, MgO, and MgS are from ref 52, the experimental bond distances for KOH and NaO are from ref 50, the experimental bond distance for BeO^+ is from ref 53, and the experimental bond distance for CaO is from ref 54. For KOH, we provide both bond distances (KO and OH).

3.4. Decomposition of Bond Energies. The decomposition scheme explained in the Introduction is very general; in some molecules considered here, we do not need all of the steps. When we decompose the bond forming processes for the 15 molecules considered here, we find that there are several types of bond forming processes, depending on which steps are involved; these types are listed in Table 5. Let A and B denote the lowest-energy dissociation products of molecule AB. In type 1, molecule AB is formed by two fragments, possibly charged, joining without excitation or electron transfer. In types 2a and 2b, there is electron transfer but no excitation, i.e., the valence states in the molecule are the same as the ground states of the charge-transferred species. Three of the molecules in this class (2a and 2b) involve less than half of an electron transfer; in particular, the partial atomic charge on BeF, HF, and BeO^+ is 0.46, 0.26, and 1.31, respectively, so the extent of electron transfer in these three cases is between 0.26 and 0.46. Although these values are less than 0.5, they are not negligible (and furthermore, other methods of calculating partial charges can yield even larger partial atomic charges in these cases), so we believe that in order to be considered to yield the right answer for the right reason the exchange-correlation functionals should predict a reasonably accurate value for the IP of Be, H, and Be^+, respectively, in these three cases. Including the IP of a cation in our test makes the test set more diverse and more representative of a broad class of applications, especially when we consider that partial atomic charges on metal elements are often greater than 1.0 in complex molecules.

The next type of bond forming is that when A is excited to a valence state different from the ground state of the interacting partner and then the bond is formed. For this type of process, we show in Figure 1 how we envision the LiO^- bond being formed from Li atom and O^-. First, the Li(2s) atom is excited to the Li(2p) state; the energetic cost is the first excitation energy of Li(s), which is 57.59 kcal/mol. Second, Li(2p) interacts with O^- to form the chemical bond; the energy released in this process is the interaction energy between Li(p) and O^- states, which is 100.20 kcal/mol. Therefore, BDE of LiO^- is the difference between IE and EE, as shown in Figure 1. In order to get the correct BDE of LiO^- without cancellation of errors, we have to predict the correct excitation energy of Li(2s) to Li(2p) and the interaction energy between Li(2p) and O^- states.

The final type of bond forming involves all of the possible steps, as explained for CaO in the Introduction. To recapitulate, we note that these bond forming processes involve the electron affinity (EA), ionization potential (IP), atomic excitation energy (EE), and interaction energy between two prepared states (IE).

For the bond types involving more than one step, we write

$$\text{Types 2a and 2b: BDE} = \text{EA} - \text{IP} + \text{IE} \quad (5)$$

$$\text{Type 3: BDE} = \text{IE} - \text{EE} \quad (6)$$

$$\text{Type 4: BDE} = \text{EA} - \text{IP} - \text{EE} + \text{IE} \quad (7)$$

Note that in a few cases (IPs, EEs, and EAs of atomic species), the PW6B95-D3(0) and PW6B95-D3(BJ) functionals give the same results as those with PW6B95.

We examined the state of the metal atom in every molecule, and we found that only BeO, CaO, and LiO^- have valence states

DOI: 10.1021/acs.jctc.5b00083
J. Chem. Theory Comput. 2015, 11, 2968−2983

Table 4. Mean Unsigned Errors and Mean Signed Errors of Bond Dissociation Energy over Seven SR Molecules, Eight MR Molecules, and All 15 Molecules Sorted in Order of Increasing Magnitude of the Error in the Overall MUE and MSE Columns (kcal/mol)

	MUE				MSE		
method	SR	MR	all	method	SR	MR	all
M08-HX	1.59	6.28	3.77	M06	2.90	−3.15	0.07
ωB97X-D	1.77	6.17	3.82	B97-1	0.40	−0.27	0.08
TPSS	2.72	5.29	3.92	revTPSS	−0.93	0.26	−0.37
PW6B95-D3(BJ)	2.91	5.12	3.94	PW6B95-D3(BJ)	−0.77	−0.19	−0.50
OreLYP	2.21	5.94	3.95	ωB97X	2.05	−3.54	−0.56
PW6B95-D3(0)	2.93	5.17	3.97	ωB97X-D	−0.19	−1.08	−0.61
PW6B95	2.98	5.16	4.00	M05-2X	3.40	−2.47	0.66
revTPSS	2.56	6.08	4.20	PW6B95-D3(0)	−0.89	−0.49	−0.70
OLYP	2.40	6.31	4.22	PW6B95	−0.96	−0.51	−0.75
τ-HCTHhyb	3.26	5.49	4.30	B3LYP	0.08	−1.99	−0.89
GAM	2.05	6.93	4.32	CAM-B3LYP	1.77	−4.03	−0.94
O3LYP	2.81	6.06	4.33	M08-HX	−0.04	−2.08	−0.99
N12-SX	2.16	6.93	4.39	O3LYP	−1.65	−0.29	−1.02
MOHLYP	4.60	4.51	4.56	OLYP	−0.71	3.02	1.03
B97-1	2.57	7.18	4.72	revB3LYP	0.82	−3.37	−1.13
M06	3.35	6.36	4.75	N12-SX	0.64	2.07	1.31
M05	2.55	7.50	4.86	GAM	1.56	1.26	1.42
B1LYP	4.50	5.39	4.91	OreLYP	0.08	3.02	1.45
PBE0	4.12	6.06	5.03	M05	−0.55	−2.72	−1.56
B97-3	2.71	7.71	5.04	B3LYP*	2.00	1.14	1.60
HSE06	4.48	5.77	5.08	B97-3	0.03	−3.52	−1.63
B3LYP*	3.35	7.10	5.10	τ-HCTHhyb	2.44	0.94	1.74
ωB97X	3.31	7.36	5.20	TPSS	0.50	3.22	1.77
M05-2X	4.00	6.65	5.24	N12	−3.75	0.38	−1.82
B3LYP	3.49	7.27	5.25	HSE06	−2.70	−1.00	−1.91
M06-2X	2.37	8.99	5.46	ωB97	2.88	0.87	1.94
revB3LYP	3.49	7.95	5.57	MOHLYP	−3.90	−0.02	−2.09
M08-SO	2.52	9.11	5.59	MPWB1K	−4.88	0.90	−2.18
CAM-B3LYP	3.20	8.85	5.84	M06-2X	0.64	−6.48	−2.68
MPW1B95	3.27	9.02	5.95	PBE0	−2.37	−3.67	−2.97
B1B95	3.32	9.02	5.98	B1LYP	−2.77	−3.62	−3.16
MPWLYP1M	4.66	7.52	6.00	TPSSh	−5.53	−0.54	−3.20
SOGGA11-X	3.75	8.83	6.12	M11	4.44	2.30	3.44
ωB97	3.96	8.59	6.12	MN12-L	−0.88	8.75	3.61
BLYP	4.37	8.53	6.31	M08-SO	−1.18	−6.75	−3.78
M11	4.58	8.29	6.31	SOGGA11-X	−3.27	−5.17	−4.16
PBE	3.90	9.20	6.38	MPW1B95	−1.96	−7.39	−4.50
N12	6.05	7.39	6.68	B1B95	−2.38	−6.98	−4.52
TPSSh	6.95	6.69	6.83	M06-L	4.65	4.60	4.63
M06-L	6.52	7.58	7.01	MPWLYP1M	3.58	5.83	4.63
BB95	4.19	10.55	7.16	BLYP	3.13	6.46	4.68
MN12-L	3.78	12.88	8.02	MN12-SX	−3.15	−7.30	−5.09
BB1K	4.92	11.67	8.07	PBE	3.11	8.98	5.85
SOGGA11	5.67	12.02	8.63	BB1K	−5.07	−9.16	−6.98
MN12-SX	7.71	9.83	8.70	BB95	3.95	10.55	7.03
MPWB1K	4.94	13.27	8.83	SOGGA11	4.15	12.02	7.82
MPW1K	6.83	13.97	10.16	MPW1K	−6.95	−11.38	−9.02
SOGGA	6.89	14.37	10.38	SOGGA	6.74	14.37	10.30
OHLYP	12.44	10.92	11.73	revTPSSh	−11.92	−8.70	−10.42
M11-L	11.96	11.48	11.74	OHLYP	−12.59	−9.41	−11.10
revTPSSh	12.62	12.02	12.34	M11-L	−12.11	−11.48	−11.82
HFLYP	16.08	25.68	20.56	HFLYP	−16.23	−21.24	−18.57
GVWN5	18.88	24.33	21.42	GVWN5	18.73	24.33	21.34
Hartree−Fock	41.14	40.81	40.98	Hartree−Fock	−41.29	−37.58	−39.56

different from their atomic ground state. For the other 12 molecules containing a metal atom, the valence state of the metal is the same as its ground state. For BeO, the chemical bond with O^- involves the p orbital of Be^+; for CaO, the chemical bond

DOI: 10.1021/acs.jctc.5b00083
J. Chem. Theory Comput. 2015, 11, 2968−2983

Table 5. Types of Bond-Forming Processes[a]

type	steps	cases
1	$A + B^- \rightarrow AB^-$	KO^-
		NaO^-
2a	$A \rightarrow A^+$	BeF
	$B \rightarrow B^-$	HF
	$A^+ + B^- \rightarrow AB$	KF
		KOH
		LiF
		LiO radical
		MgO
		MgS
		NaO radical
2b	$A^+ \rightarrow A^{2+}$	BeO^+
	$B \rightarrow B^-$	
	$A^{2+} + B^- \rightarrow AB^+$	
3	$A(G) \rightarrow A(V)$	LiO^-
	$A(V) + B^- \rightarrow AB^-$	
4	$A \rightarrow A^+$	BeO
	$A^+(G) \rightarrow A^+(V)$	CaO
	$B \rightarrow B^-$	
	$A^+(V) + B^- \rightarrow AB$	

[a]G denotes ground electronic state; V denotes valence state.

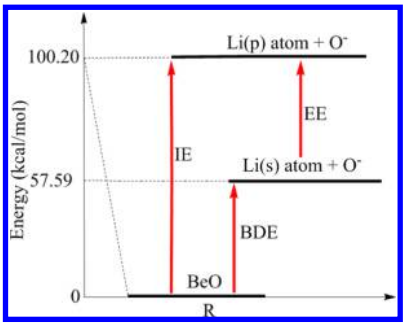

Figure 1. Decomposition of bond dissociation energy of LiO^-.

involves $Ca^+(d)$; and for LiO^-, the chemical bond involves mainly Li(p). Therefore, we can envision the formation of a chemical bond in these molecules as proceeding by exciting an electron of Be^+ from the 2s orbital to the 2p orbital, an electron of Ca^+ from the 4s orbital to the 3d orbital, and an electron of Li from the 2s orbital to the 2p orbital. We found that the Hartree−Fock method gives the smallest error for these three monatomic excitation energies, with an MUE of 1.69 kcal/mol. The best 18 exchange-correlation functionals for atomic excitation energies in Table 6 are hybrid functionals, whereas SOGGA11 and N12 are the best GGAs in terms of smallest mean unsigned error for excitation energy for these three atoms. Most of the exchange-correlation functionals underestimate the excitation energy; thus, we see in Table 6 that all of the exchange-correlation functionals give a negative MSE for excitation energy. Proceeding from the Hartree−Fock method to HFLYP, the error goes from 1.59 to −0.23 kcal/mol. Therefore, the Hartree−Fock exchange tends to lower the energy of s orbitals more than p and d orbitals; on the other hand, correlation tends to lower the energy of p and d orbitals more than s orbitals.

Table 6 shows the MUE and MSE of the ionization potential over eight data (Be, Ca, Be^+, H, K, Li, Mg, and Na), as well as atomic excitation energy over three data (Be, Ca+, and Li) and MUE and MSE over all 11of these data (8IP and 3EE). Since some of the 15 molecules have the same ionization potential, like MgO and MgS, we count that IP only once in the table. The columns labeled IP show that revTPSS gives the smallest error overall, which is 2.27 kcal/mol, the second best is B97-3, with a MUE of 2.29 kcal/mol, and the third best is B97-1, with a MUE of 2.57 kcal/mol. The columns labeled all show that, surprisingly, HFLYP (with 100% Hartree−Fock exchange) gives the smallest error overall (3.30 kcal/mol) by a considerable margin, the second best is M06-2X, with a MUE of 4.01 kcal/mol, and the third best is MPWB1K, with a MUE of 4.11 kcal/mol.

Table 7 shows the MUE and MSE of electron affinity for all molecules. The columns labeled all include the electron affinity of O, F, OH, and S. Table 7 shows that TPSS, PW6B95, PW6B95-D3(0), and PW6B95-D3(BJ) give the smallest overall error, which is 0.97 kcal/mol, followed by O3LYP and M08-HX, with errors of 0.99 and 1.08 kcal/mol, respectively. Five of the methods give errors larger than 10 kcal/mol for electron affinity. Thirty-five of the 54 methods in Table 7 have a negative MSE for electron affinity; the systematic underestimation of electron affinity by most exchange-correlation functions is a serious concern.

Table 8 shows the MUE and MSE of the interaction energy (as defined above) for all molecules, single-reference systems, and multireference systems. The columns labeled all include all 15 molecules. The SR columns include seven single-reference diatomic molecules and one triatomic molecule, which are BeF radical, BeO^+, HF, KF, KOH, LiF, LiO radical, and NaO radical. The MR columns include seven diatomic molecules, which are BeO, CaO, LiO^-, NaO^-, KO^-, MgO and MgS. Table 8 shows that τ-HCTHhyb gives the smallest overall error of 3.59 kcal/mol, followed by MN12-SX, GAM, TPSS, and M05-2X, with errors of 3.71, 3.86, 4.16, and 4.33 kcal/mol, respectively. We find that MN12-SX gives the smallest error of interaction energy for single-reference systems and τ-HCTHhyb gives the smallest error of interaction energy for multireference systems. By comparing both SR and MR columns, we found that τ-HCTHhyb, MN12-SX, GAM, and M05-2X are best for predicting the interaction energy for both multireference and single-reference systems. Forty-eight of the 54 methods in Table 8 have a negative MSE in the interaction energy.

In Table 9, we show average mean unsigned errors (AUE), where average refers to averaging over all data (IPs, EEs, EAs, IEs, and BDEs), whereas we have used the word mean for averaging over all of the molecules for a particular kind of data. Note that since the IE is equal to the BDE for the two type-1 cases we do not include the IE in those cases in order to avoid including it twice. From Table 9, we can see that multireference systems are much harder to predict than single-reference systems. Table 9 shows that PW6B95-D3(BJ) and revTPSS give the smallest overall AUE of 4.05 kcal/mol, followed by TPSS, PW6B95-D3(0), PW6B95, M08-HX, M05-2X, B97-1, and τ-HCTHhyb. Adding dispersion corrections to density functional PW6B95 reduces the overall AUE by 0.09 and 0.06 kcal/mol for D3(BJ) and D3(0), respectively. By comparing the SR and MR columns, we find that the functionals that predict good results for both multireference and single-reference systems are PW6B95-D3(0), PW6B95-D3(BJ), PW6B95, revTPSS, M08-HX, TPSS, B97-1, τ-HCTHhyb, and M05-2X.

It is sometimes stated (erroneously) that parametrized functionals do not perform well outside of their training set. The literature is replete with counterexamples, but the present study provides an excellent opportunity to discuss this because eight of the 10 best performing functionals in Table 9 are parametrized against experimental data. One can ask, how many of these 15 bond energies were used in their parametrization? In

DOI: 10.1021/acs.jctc.5b00083
J. Chem. Theory Comput. 2015, 11, 2968−2983

Table 6. Mean Unsigned Errors and Mean Signed Errors of Ionization Potentials (Eight Data: Be, Be^+, Ca, H, K, Li, Mg, and Na) and Excitation Energies (Three Data: Li, Be^+, and Ca^+) Sorted in Order of Increasing Magnitude of the Error on All 11 Data

	MUE (kcal/mol)				MSE (kcal/mol)		
method	IP	EE	all	method	IP	EE	all
HFLYP	3.78	2.02	3.30	M08-HX	2.74	−6.62	0.18
M06-2X	3.86	4.42	4.01	SOGGA11-X	1.86	−6.26	−0.35
MPWB1K	3.51	5.70	4.11	M08-SO	2.87	−6.28	0.37
M08-HX	3.28	6.62	4.19	CAM-B3LYP	1.98	−6.82	−0.42
PW6B95	3.05	7.31	4.21	B3LYP	2.78	−9.15	−0.47
PW6B95-D3(0)	3.05	7.31	4.21	B3LYP*	2.74	−9.53	−0.61
PW6B95-D3(BJ)	3.05	7.31	4.21	M05-2X	1.70	−7.81	−0.89
M05	2.98	7.52	4.22	revB3LYP	2.01	−8.89	−0.96
M08-SO	3.53	6.28	4.28	MPWLYP1M	2.15	−9.86	−1.12
MPW1B95	3.39	7.03	4.38	MN12-SX	2.72	−1.70	1.51
BB1K	3.77	6.09	4.40	PBE	1.77	−10.47	−1.57
CAM-B3LYP	3.69	6.82	4.54	PW6B95	0.56	−7.31	−1.59
B97-3	2.29	10.86	4.62	PW6B95-D3(0)	0.56	−7.31	−1.59
M05-2X	3.49	7.81	4.67	PW6B95-D3(BJ)	0.56	−7.31	−1.59
B97-1	2.57	10.38	4.70	M06-2X	−0.70	−4.42	−1.71
revTPSS	2.27	11.24	4.71	M11-L	4.02	−4.13	1.80
B1B95	3.60	7.87	4.76	OreLYP	1.78	−11.99	−1.98
B1LYP	3.54	8.40	4.87	τ-HCTHhyb	2.09	−12.92	−2.00
MPW1K	3.92	7.50	4.90	BLYP	1.25	−11.29	−2.17
TPSSh	2.71	10.75	4.90	M05	−0.17	−7.52	−2.17
HSE06	3.55	8.83	4.99	HFLYP	−3.06	−0.23	−2.29
SOGGA11-X	4.53	6.26	5.00	B1LYP	−0.04	−8.40	−2.32
M11	3.64	8.67	5.01	HSE06	0.09	−8.83	−2.34
revB3LYP	3.67	8.89	5.09	B97-1	0.62	−10.38	−2.38
PBE0	3.55	9.30	5.12	PBE0	0.09	−9.30	−2.47
TPSS	2.69	11.78	5.17	O3LYP	0.20	−10.60	−2.74
ωB97X	4.72	7.07	5.36	MPW1K	−0.97	−7.50	−2.75
O3LYP	3.42	10.60	5.37	B97-3	0.07	−10.86	−2.91
N12-SX	3.53	10.41	5.41	SOGGA11	7.39	−8.91	2.95
PBE	3.51	10.47	5.41	MPW1B95	−1.48	−7.03	−2.99
OreLYP	2.94	11.99	5.41	MPWB1K	−2.21	−5.70	−3.16
B3LYP*	4.04	9.53	5.54	TPSS	−0.28	−11.78	−3.42
MPWLYP1M	3.96	9.86	5.57	TPSSh	−0.73	−10.75	−3.46
MOHLYP	3.51	11.06	5.57	revTPSS	−0.68	−11.24	−3.56
B3LYP	4.28	9.15	5.60	M11	−1.64	−8.67	−3.56
ωB97X-D	4.07	10.02	5.69	revTPSSh	0.50	−14.42	−3.57
BLYP	3.66	11.29	5.74	OLYP	−0.58	−11.82	−3.64
ωB97	4.40	9.60	5.82	ωB97	−1.43	−9.60	−3.66
SOGGA	4.27	10.61	6.00	B1B95	−2.24	−7.87	−3.78
BB95	4.11	11.15	6.03	BB1K	−2.94	−6.09	−3.80
OLYP	3.99	11.82	6.13	GAM	−0.18	−13.64	−3.85
revTPSSh	3.23	14.42	6.28	MOHLYP	−1.37	−11.06	−4.01
τ-HCTHhyb	3.82	12.92	6.30	GVWN5	2.64	−21.77	−4.02
M06	4.26	12.88	6.61	ωB97X	−2.93	−7.07	−4.05
GAM	4.33	13.64	6.87	BB95	−1.56	−11.15	−4.18
SOGGA11	7.08	8.91	7.58	SOGGA	−1.81	−10.61	−4.21
OHLYP	6.92	11.10	8.06	N12-SX	−2.01	−10.41	−4.30
M11-L	6.43	12.63	8.12	ωB97X-D	−2.43	−10.02	−4.50
N12	8.37	9.13	8.58	N12	−2.95	−9.13	−4.64
Hartree−Fock	11.46	1.69	8.79	M06	−1.82	−12.88	−4.84
GVWN5	4.58	21.77	9.27	MN12-L	−2.06	−18.88	−6.65
MN12-L	7.86	18.88	10.87	OHLYP	−6.86	−11.10	−8.01
MN12-SX	8.81	17.29	11.12	M06-L	−3.93	−27.40	−10.33
M06-L	7.86	27.40	13.19	Hartree−Fock	−15.83	1.59	−11.08

general, the answer is very few. The parametrization of M08-HX involved HF but none of the 14 metal-containing molecules. In fact, the only two metal-containing molecules used in parametrizing M08-HX were AlF_3 and $AlCl_3$. The parametrization of M05 and M05-2X also involved only HF from the present set; however, it involved six metal-containing compounds: AlF_3,

DOI: 10.1021/acs.jctc.5b00083
J. Chem. Theory Comput. 2015, 11, 2968−2983

$AlCl_3$, and four transition-metal−ligand bond energies. Parametrization of PW6B95 involved none of the 15 molecules studied here, and, in fact, it involved no bonds involving metals. Parametrization of B97-1 involved HF and five metal-containing compounds: LiH, Li_2, LiF, Na_2, and NaCl. Only τ-HCTHhyb involved significant amounts of metal data, and it also involved HF; for the metal-containing data, it involved six molecules containing Li, four with Na, five with Be, three with Mg, five with Al, one with Ni, two with Fe, and three with Cr; five of these molecules (HF, LiF, BeO, BeF, and MgO) overlap the present 15-molecule test set.

The revB3LYP functional is a modification of the B3LYP functional by adding organic molecules to the training set.[38] The GAM functional is a modification of the N12 functional by adding transition metals and other various molecules to the training set and smoothness constraints.[37] Table 9 shows that GAM is the best GGA and has a large improvement (from 6.50 to 4.59 kcal/mol) from N12; however, the performance of revB3LYP and B3LYP is almost the same. Therefore, in order to obtain good functionals to deal with systems in the present article, we do need to include more diverse data, especially metals into the training set.

In order to predict which molecule is the hardest to model, we calculate the MUE of each molecule with respect to the 54 methods. As we can see from Table 10, the molecule that has largest MUE is LiO^-, and the one with smallest MUE is HF. All of the single-reference molecules have a smaller MUE than the multireference molecules, except that MgS has an MUE smaller than BeO^+ and BeF and MgO has an MUE smaller than BeO^+. Also, we found that molecules that require an excitation process to make the valence state of the chemical bond have a larger MUE; in particular, CaO, BeO, and LiO^- are in the last four molecules of Table 10. We can explain this by the fact that most functionals do not predict the excitation energy very well, and our breakdown shows that this is the main source of error for these three molecules.

In Table 11, we show the AUE of each functional and arrange them according to the classification of exchange-correlation functionals. For all 15 molecules, the best gradient approximation is GAM and the best meta-GGA is revTPSS; the best hybrid GGA is B97-1, and the best hybrid meta-GGA is PW6B95, followed by M08-HX. If we restrict attention to the eight single-reference molecules, the best GGA is OLYP, the best meta-GGA is revTPSS, the best hybrid GGA is B97-1, and the best hybrid meta-GGA is M08-HX. For the seven multireference molecules, the best GGA is OreLYP, the best meta-GGA is TPSS, the best hybrid GGA is MPWLYP1W, and the best hybrid meta-GGA is PW6B95, followed by M08-HX. The good results for the M08-HX functional, which has 52.23% Hartree−Fock exchange, may be considered surprising since it has been known for a long time that B3LYP (with 20% Hartree−Fock exchange) is better than BHLYP (which has 50% Hartree−Fock exchange) for transition metal bond energies.[44] We show the 22 best functionals (using the ranking of Table 9) in Figure 2. For most of the functionals, the biggest error comes from the excitation energy, which is above 6 kcal/mol. The AUE for BDE, EE, IE, IP, and EA is about 4.2 kcal/mol. Among all 22 functionals in Figure 2, M06-2X is the only one that has all four errors below 6 kcal/mol. Most functionals shown in Figure 2 give a large error of EE and small errors of BDE, IE, and EA. Therefore, the overall small MUEs for molecule requiring an excitation to achieve their valence state come from cancellation of errors. In trying to design a good functional, we should try to get all five components right. From Figure 2, the only functional that gives relatively correct values for all five components is M06-2X.

We computed the Pearson correlation coefficient r between the MUE of the BDE and the MUE in each of the four

Table 7. Mean Unsigned Errors and Mean Signed Errors (kcal/mol) of Electron Affinity of F, O, OH, and S.

method	MUE of EA	method	MSE of EA
PW6B95	0.97	O3LYP	0.03
PW6B95-D3(0)	0.97	M05-2X	−0.09
PW6B95-D3(BJ)	0.97	MOHLYP	−0.11
TPSS	0.97	TPSS	−0.21
O3LYP	0.99	ωB97X-D	−0.43
M08-HX	1.08	PW6B95	−0.61
M05-2X	1.10	PW6B95-D3(0)	−0.61
B97-1	1.30	PW6B95-D3(BJ)	−0.61
MOHLYP	1.43	B97-1	−0.71
revTPSS	1.47	M08-HX	0.74
ωB97X-D	1.49	OLYP	0.89
B97-3	1.68	B97-3	−0.95
GAM	1.71	ωB97X	0.99
OLYP	1.75	GAM	−1.42
M11	1.76	revTPSS	−1.47
M06	1.91	ωB97	−1.51
M06-2X	1.94	M06-2X	−1.60
τ-HCTHhyb	2.05	M11	1.76
ωB97	2.10	M06	−1.91
M08-SO	2.21	SOGGA11-X	−2.03
revB3LYP	2.22	τ-HCTHhyb	2.05
ωB97X	2.26	revB3LYP	2.15
B1LYP	2.34	SOGGA	2.19
SOGGA	2.35	M08-SO	2.21
CAM-B3LYP	2.39	CAM-B3LYP	2.27
N12-SX	2.44	B1LYP	−2.34
TPSSh	2.54	N12-SX	−2.44
HSE06	2.62	TPSSh	−2.54
PBE0	2.72	HSE06	−2.62
M05	2.78	PBE0	−2.72
SOGGA11-X	2.82	M05	−2.78
B3LYP	2.86	N12	−2.85
OreLYP	2.95	B3LYP	2.86
N12	3.17	OreLYP	2.95
MN12-SX	3.18	MN12-SX	−3.05
MPW1B95	3.22	MPW1B95	−3.22
B1B95	3.27	B1B95	−3.27
revTPSSh	3.67	revTPSSh	−3.67
B3LYP*	4.14	B3LYP*	4.14
BB95	4.47	BB95	4.47
MPWLYP1M	4.51	MPWLYP1M	4.51
PBE	4.61	PBE	4.61
BLYP	4.77	M11-L	−4.70
M06-L	4.89	BLYP	4.77
MPWB1K	6.63	M06-L	−4.89
BB1K	6.80	MPWB1K	−6.63
MPW1K	7.15	BB1K	−6.80
MN12-L	7.82	MPW1K	−7.15
M11-L	7.94	MN12-L	−7.54
OHLYP	10.42	OHLYP	−10.42
SOGGA11	11.52	SOGGA11	11.52
GVWN5	12.56	GVWN5	12.56
HFLYP	19.64	HFLYP	−19.64
Hartree−Fock	43.50	Hartree−Fock	−43.50

DOI: 10.1021/acs.jctc.5b00083
J. Chem. Theory Comput. 2015, 11, 2968−2983

Table 8. Mean Unsigned Errors and Mean Signed Errors of Interaction Energy between Prepared Valence States for Eight SR Molecules, Seven MR Molecules, and All 15 Molecules Sorted in Order of Increasing Magnitude of the Error in the Overall MUE and MSE Columns

	MUE (kcal/mol)				MSE (kcal/mol)		
method	SR	MR	all	method	SR	MR	all
τ-HCTHhyb	2.84	4.44	3.59	M05-2X	1.75	−2.61	−0.28
MN12-SX	2.14	5.50	3.71	MPWB1K	2.34	−1.32	0.63
GAM	2.55	5.35	3.86	M08-HX	2.47	−4.42	−0.75
TPSS	3.45	4.97	4.16	ωB97	−0.25	−1.69	−0.92
M05-2X	2.72	6.18	4.33	MPWLYP1M	0.06	−2.63	−1.20
MPWLYP1M	4.47	4.73	4.59	TPSS	1.34	−4.25	−1.27
revTPSS	3.07	6.46	4.65	PW6B95-D3(BJ)	1.47	4.90	−1.50
SOGGA	3.31	6.20	4.66	M11	0.62	−4.14	−1.60
PW6B95-D3(BJ)	2.92	7.31	4.97	M05	1.17	−4.87	−1.65
PW6B95-D3(0)	2.92	7.52	5.06	PW6B95-D3(0)	1.36	−5.21	−1.71
OreLYP	5.27	4.90	5.09	N12-SX	0.45	−4.28	−1.76
BLYP	4.69	5.57	5.10	PBE	2.99	0.66	1.90
PW6B95	2.96	7.97	5.30	GAM	−1.59	−2.30	−1.92
PBE	4.74	6.03	5.35	PW6B95	1.29	−5.68	−1.96
B97-1	2.99	8.06	5.35	HSE06	1.80	−6.36	−2.01
N12-SX	2.77	8.52	5.45	τ-HCTHhyb	0.00	−4.31	−2.01
HSE06	2.57	9.12	5.63	SOGGA11-X	1.91	−6.75	−2.13
BB95	6.01	5.33	5.70	B97-1	0.55	−5.25	−2.16
B3LYP*	3.57	8.14	5.70	MN12-SX	0.37	−5.18	−2.22
M05	3.54	8.25	5.74	MN12-L	0.31	4.53	2.28
M06	2.58	9.38	5.75	BB95	−4.29	−0.14	−2.35
M08-HX	3.37	8.62	5.82	SOGGA11	−0.35	5.52	2.39
OLYP	5.13	6.71	5.86	HFLYP	8.00	−14.40	−2.45
N12	4.01	8.02	5.88	OreLYP	−1.91	−3.19	−2.51
O3LYP	4.28	8.08	6.06	BLYP	−1.77	−3.60	−2.62
M11	2.76	10.26	6.26	SOGGA	1.03	4.48	2.64
revB3LYP	3.50	9.98	6.52	revTPSS	0.04	−5.71	−2.64
B3LYP	3.51	10.14	6.60	B3LYP*	0.42	−6.43	−2.78
SOGGA11-X	3.28	10.40	6.61	M06-L	0.74	−7.07	−2.90
M11-L	3.38	10.48	6.69	N12	0.94	−7.70	−3.09
ωB97	4.53	9.23	6.72	OLYP	−1.91	−5.15	−3.42
B1LYP	3.66	10.30	6.76	O3LYP	−0.61	−6.78	−3.49
B97-3	3.12	10.91	6.76	CAM-B3LYP	1.58	−9.57	−3.62
M06-L	2.21	11.97	6.76	B3LYP	0.56	−8.62	−3.72
ωB97X-D	2.92	11.29	6.83	B1LYP	0.76	−8.86	−3.73
MPW1B95	2.69	11.79	6.94	M06-2X	−0.46	−7.56	−3.77
MOHLYP	6.49	7.59	7.00	M11-L	1.70	−10.48	−3.99
MN12-L	2.86	12.01	7.13	revB3LYP	0.98	−9.98	−4.13
PBE0	4.49	10.24	7.17	M06	0.06	−9.38	−4.34
SOGGA11	7.47	7.07	7.28	B97-3	−0.51	−8.79	−4.38
CAM-B3LYP	3.71	11.36	7.28	TPSSh	−2.81	−6.32	−4.45
B1B95	3.00	12.30	7.34	M08-SO	0.55	−10.33	−4.53
M08-SO	2.72	12.69	7.37	BB1K	1.48	−11.92	−4.77
TPSSh	6.64	8.34	7.43	MPW1B95	1.28	−11.79	−4.82
M06-2X	5.53	9.64	7.44	MPW1K	2.99	−14.19	−5.03
MPWB1K	2.94	13.43	7.84	PBE0	−1.43	−9.91	−5.39
BB1K	2.95	14.44	8.31	GVWN5	3.48	7.87	5.53
ωB97X	4.50	13.38	8.64	ωB97X-D	−2.85	−8.60	−5.54
MPW1K	3.09	16.78	9.48	B1B95	0.09	−12.30	−5.70
GVWN5	5.92	14.55	9.95	MOHLYP	−5.08	−7.59	−6.25
OHLYP	6.83	16.23	11.21	ωB97X	−4.50	−11.44	−7.74
revTPSSh	12.48	13.07	12.76	OHLYP	−5.39	−16.23	−10.45
HFLYP	8.00	18.83	13.05	revTPSSh	−8.37	−13.07	−10.56
Hartree−Fock	3.85	30.44	16.26	Hartree−Fock	1.29	−27.22	−12.01

components of BDE. The Pearson correlation coefficient is a measurement of the correlation between two variables X and Y; its value varies from −1 to 1, where −1 means perfect anticorrelation between X and Y, 1 means perfect positive

DOI: 10.1021/acs.jctc.5b00083
J. Chem. Theory Comput. 2015, 11, 2968−2983

Table 9. Values of the Average Mean Unsigned Errors (AUE) over 25 Energetic Data[a] from Eight SR Molecules, 20 Energetic Data[b] from Seven MR Molecules, and 43 Energetic Data[c] for All 15 Molecules Sorted by Last Column

	AUE (kcal/mol)					
method	SR value	SR rank	MR value	MR rank	overall value	overall rank
PW6B95-D3(BJ)	2.86	11	5.21	1	4.05	1
revTPSS	2.56	2	5.85	6	4.05	2
TPSS	2.75	7	5.68	4	4.08	3
PW6B95-D3(0)	2.87	13	5.28	2	4.08	4
PW6B95	2.85	10	5.39	3	4.14	5
M08-HX	2.46	1	6.02	7	4.18	6
M05-2X	2.73	6	6.10	8	4.34	7
B97-1	2.64	3	6.47	12	4.37	8
τ-HCTHhyb	2.98	14	6.12	10	4.42	9
M05	3.16	16	6.10	9	4.50	10
GAM	2.65	4	6.82	18	4.59	11
OreLYP	3.61	23	5.72	5	4.63	12
N12-SX	2.86	12	7.26	25	4.70	13
O3LYP	3.30	18	6.81	16	4.93	14
B97-3	2.71	5	7.57	32	4.94	15
HSE06	3.60	21	6.81	17	5.03	16
OLYP	3.60	22	6.78	15	5.03	17
M06-2X	3.80	27	6.54	13	5.08	18
ωB97X-D	2.76	8	8.06	37	5.09	19
M06	3.36	19	7.36	28	5.14	20
M08-SO	2.77	9	7.82	34	5.15	21
MPW1B95	3.15	15	7.86	36	5.20	22
B3LYP*	3.95	30	6.86	19	5.21	23
M11	3.46	20	7.45	29	5.33	24
CAM-B3LYP	3.62	24	7.49	31	5.37	25
MPWLYP1M	4.80	40	6.26	11	5.37	26
B1LYP	3.92	29	7.10	21	5.38	27
B3LYP	3.85	28	7.30	27	5.40	28
revB3LYP	3.64	25	7.28	26	5.42	29
B1B95	3.24	17	8.39	39	5.49	30
PBE0	4.10	31	7.17	22	5.49	31
MOHLYP	4.56	37	6.64	14	5.54	32
ωB97	4.14	33	7.45	30	5.55	33
PBE	4.47	36	7.20	24	5.60	34
SOGGA11-X	3.77	26	7.79	33	5.68	35
BLYP	4.71	39	7.18	23	5.70	36
BB95	4.96	41	7.83	35	6.15	37
ωB97X	4.13	32	8.92	41	6.18	38
TPSSh	5.37	43	7.03	20	6.20	39
N12	5.52	45	8.21	38	6.50	40
SOGGA	4.60	38	9.10	43	6.54	41
BB1K	4.27	35	9.89	45	6.68	42
MN12-SX	5.78	46	8.67	40	7.10	43
MPWB1K	4.25	34	11.12	48	7.25	44
MPW1K	5.19	42	11.20	50	7.87	45
MN12-L	5.45	44	11.19	49	7.96	46
SOGGA11	7.49	49	8.96	42	8.09	47
M06-L	5.92	47	10.87	46	8.19	48
M11-L	7.34	48	10.93	47	9.08	49
revTPSSh	9.15	51	9.44	44	9.49	50
OHLYP	8.53	50	13.45	51	10.58	51
GVWN5	10.96	52	17.17	52	13.88	52
HFLYP	11.44	53	17.38	53	14.04	53
Hartree−Fock	22.04	54	32.17	54	26.00	54

[a]Eight IP, three EA, six IE, and eight BDE. [b]Three IP, two EA, three EE, five IE and seven BDE. [c]Eight IP, four EA, three EE, 13 IE, 15 BDE.

Table 10. Mean Unsigned Errors (MUE) of Bond Distances (Å) of 12 Molecules over 54 methods and Mean Unsigned Errors of Energies (BDE, IP, EA, EE, and IE) of All 15 Molecules over 54 methods Sorted in Order of Increasing Magnitude of the Error of Energies (kcal/mol)

method	bond distances	energies
HF	0.006	3.81
NaO	0.029	3.98
LiF	0.008	4.11
LiO	0.016	4.25
KF	0.023	4.41
KOH[a]	0.013, 0.044	4.78
MgS	0.012	5.25
BeF	0.007	5.59
MgO	0.020	6.66
BeO^+	0.014	6.91
NaO^-		8.12
BeO	0.047	8.67
KO^-		9.24
CaO	0.025	9.31
LiO^-		9.54

[a]The MUE for KO bond in KOH is 0.013 Å, and the MUE for OH bond in KOH is 0.044 Å

correlation between X and Y, and zero means no correlation between X and Y. We found that the correlation coefficients between the MUE of BDE and the MUEs of IP, EA, EE, and IE are 0.59, 0.95, −0.11, and 0.82, respectively. Therefore, the MUE of the BDE is significantly positively correlated with the MUE of EA and IE, but, perhaps surprisingly, it is slightly anticorrelated with the MUE of EE. The high correlation of the MUEs of the EA and IE with the MUE of BDE shows that in order to get the correct BDE we should get the both EA of the nonmetal atoms and the IE between two prepared states correctly. This is perhaps not so surprising, but the relative magnitudes of the four correlation coefficients could not have been anticipated without numerical data.

3.5. Dipole Moments. In order to see the correlation between charge distribution and bond dissociation energy, we studied the dipole moments of all 15 molecules. Table 12 shows the MUE and MSE of dipole moment predicted by 53 exchange-correlation functionals and the Hartree−Fock method. The best six exchange-correlation functionals for predicting the dipole moments are MPWLYP1M, PBE, O3LYP, SOGGA, MOHLYP, and PW6B95-D3(0). However, among these functionals, only MOHLYP, O3LYP, and PW6B95-D3(0) are within the best 10 for BDE.

We also calculated the correlation between the MUE in the dipole moments and the MUEs of the IP, EA, and BDE. The values of the Pearson correlation coefficients for these three correlations are r = 0.40, 0.65, and 0.58, respectively. This shows that the MUE of the electron affinity has the largest correlation with the MUE of the dipole moment, which, in turn, implies that the errors in the predictions of dipole

DOI: 10.1021/acs.jctc.5b00083
J. Chem. Theory Comput. 2015, 11, 2968−2983

Table 11. Average Mean Unsigned Errors (AUE) over 25 Energetic Data (8IP, 3EA, 6IE, and 8BDE) from Eight SR Molecules, 20 Energetic Data (3IP, 2EA, 3EE, 5IE, and 7BDE) from Seven MR Molecules, and 43 Energetic Data (8IP, 4EA, 3EE, 13IE, and 15BDE) from All 15 Molecules Arranged by Type of Functional and Sorted in Order of Increasing Magnitude of the Overall Error (kcal/mol) for Each Type

		AUE		
type	method	SR	MR	all
LSDA	GVWN5	10.96	17.17	13.88
GGA	OreLYP	3.61	5.72	4.63
	OLYP	3.60	6.78	5.03
	MOHLYP	4.56	6.64	5.54
	PBE	4.47	7.20	5.60
	BLYP	4.71	7.18	5.70
	BB95	4.96	7.83	6.15
	SOGGA	4.60	9.10	6.54
	SOGGA11	7.49	8.96	8.09
	OHLYP	8.53	13.45	10.58
	HFLYP	11.44	17.38	14.04
NGA	GAM	2.65	6.82	4.59
	N12	5.52	8.21	6.50
meta-GGA	revTPSS	2.56	5.85	4.05
	TPSS	2.75	5.68	4.08
	M06-L	5.92	10.87	8.19
	M11-L	7.34	10.93	9.08
meta-NGA	MN12-L	5.45	11.19	7.96
global hybrid GGA	B97-1	2.64	6.47	4.37
	O3LYP	3.30	6.81	4.93
	B97-3	2.71	7.57	4.94
	B3LYP*	3.95	6.86	5.21
	MPWLYP1M	4.80	6.26	5.37
	B1LYP	3.92	7.10	5.38
	B3LYP	3.85	7.30	5.40
	revB3LYP	3.64	7.28	5.42
	B1B95	3.24	8.39	5.49
	PBE0	4.10	7.17	5.49
	SOGGA11-X	3.77	7.79	5.68
	MPW1K	5.19	11.20	7.87
global hybrid meta-GGA	PW6B95	2.85	5.39	4.14
	M08-HX	2.46	6.02	4.18
	M05-2X	2.73	6.10	4.34
	τ-HCTHhyb	2.98	6.12	4.42
	M05	3.16	6.10	4.50
	M06-2X	3.80	6.54	5.08
	M06	3.36	7.36	5.14
	M08-SO	2.77	7.82	5.15
	MPW1B95	3.15	7.86	5.20
	TPSSh	5.37	7.03	6.20
	BB1K	4.27	9.89	6.68
	MPWB1K	4.25	11.12	7.25
	revTPSSh	9.15	9.44	9.49
range-separated hybrid GGA	HSE06	3.60	6.81	5.03
	CAM-B3LYP	3.62	7.49	5.37
	ωB97	4.14	7.45	5.55
	ωB97X	4.13	8.92	6.18
range-separated hybrid NGA	N12-SX	2.86	7.26	4.70
range-separated hybrid meta-GGA	M11	3.46	7.45	5.33
range-separated hybrid meta-NGA	MN12-SX	5.78	8.67	7.10
DFT-D	PW6B95-D3(BJ)	2.86	5.21	4.05
	PW6B95-D3	2.87	5.28	4.08
	ωB97X-D	2.76	7.82	5.09

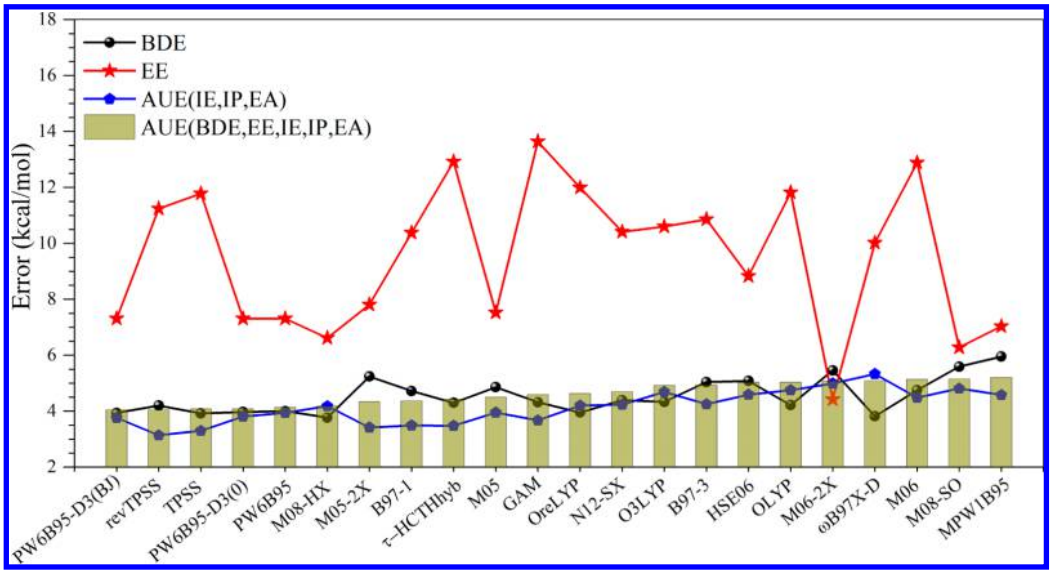

Figure 2. Average unsigned error for 22 best functionals for 15 diatomic molecules in this article. The black dot stands for the mean unsigned error of bond energies, the red star stands for the mean unsigned error of excitation energies, the blue pentagon stands for the average unsigned error of IE, IP, and EA, and the green rectangle stands for average unsigned error of BDE, EE, IE, IP, and EA.

moments by various exchange-correlation functionals tend to be dominated more by the difficulty of predicting the electron-acceptor strength than predicting the electron-donor strength. This is an important consideration when using density functional theory for charge transfer and probably also for charge transport.

3.6. Bond Distance. We also tested the bond distances of the 12 molecules that have experimental values available. All of the

DOI: 10.1021/acs.jctc.5b00083
J. Chem. Theory Comput. 2015, 11, 2968−2983

Table 12. Mean Unsigned Errors and Mean Signed Errors of Dipole Moment of All 15 Molecules Sorted in Order of Increasing Magnitude of the Error (Debye)

method	MUE	MSE
MPWLYP1M	0.43	−0.13
PBE	0.49	−0.28
O3LYP	0.50	0.20
SOGGA	0.51	−0.26
MOHLYP	0.52	0.35
PW6B95-D3(0)	0.54	0.35
PW6B95-D3(BJ)	0.54	0.04
PW6B95	0.55	0.38
B1LYP	0.57	0.32
B3LYP	0.58	0.36
revTPSS	0.58	0.20
TPSS	0.60	0.21
TPSSh	0.60	0.35
M06-L	0.64	0.41
HSE06	0.64	0.38
N12	0.66	0.09
BLYP	0.66	−0.03
τ-HCTHhyb	0.67	0.46
B3LYP*	0.67	0.33
GAM	0.68	0.35
revTPSSh	0.69	0.45
PBE0	0.71	0.56
OreLYP	0.72	−0.05
GVWN5	0.72	0.15
B97-1	0.72	0.56
MPWB1K	0.75	0.37
MN12-SX	0.75	0.62
B97-3	0.76	0.66
OHLYP	0.76	0.24
OLYP	0.77	0.00
M06	0.79	0.62
M08-SO	0.82	0.74
M08-HX	0.82	0.71
M11-L	0.82	0.55
M06-2X	0.83	0.68
M05	0.84	0.64
N12-SX	0.85	0.72
revB3LYP	0.85	0.64
B1B95	0.86	0.72
MN12-L	0.87	0.71
CAM-B3LYP	0.88	0.65
BB1K	0.88	0.59
SOGGA11-X	0.89	0.80
MPW1B95	0.93	0.77
M05-2X	0.95	0.88
ωb97X	0.96	0.83
ωB97X-D	0.98	0.86
BB95	1.00	0.31
MPW1K	1.07	0.57
SOGGA11	1.08	0.23
M11	1.08	0.84
ωB97	1.12	1.05
HFLYP	1.29	0.76
Hartree−Fock	1.63	0.47

Table 13. Mean Unsigned Errors and Mean Signed Errors of 54 Methods over 13 Geometric Data from 12 Main-Group Molecules Sorted in Order of Increasing Magnitude of MUE (Å)

name	MUE	MSE
B3LYP*	0.011	0.004
revTPSSh	0.011	0.004
revB3LYP	0.011	0.001
TPSSh	0.012	0.003
B3LYP	0.012	0.003
τ-HCTHhyb	0.012	0.008
B97-1	0.012	0.003
B1LYP	0.012	0.002
MN12-L	0.012	0.002
HSE06	0.012	−0.004
M06-L	0.013	−0.002
B1B95	0.013	−0.004
revTPSS	0.013	0.010
TPSS	0.013	0.002
MN12-SX	0.013	0.000
PBE	0.013	−0.005
M05-2X	0.013	−0.002
M08-SO	0.013	0.004
M08-HX	0.013	0.002
SOGGA11	0.013	−0.004
PW6B95-D3(BJ)	0.013	−0.004
PW6B95-D3(0)	0.013	−0.004
GAM	0.014	0.008
MPW1B95	0.014	−0.006
B97-3	0.014	0.001
PBE0	0.014	0.011
M06-2X	0.014	−0.004
M05	0.014	−0.002
N12-SX	0.015	−0.007
MPWLYP1M	0.015	0.014
SOGGA11-X	0.015	0.001
O3LYP	0.015	0.008
M06	0.015	−0.005
CAM-B3LYP	0.016	−0.007
BB95	0.016	0.015
ωB97X-D	0.017	0.000
BB1K	0.018	−0.012
ωB97X	0.018	0.000
M11	0.019	0.003
N12	0.019	−0.012
BLYP	0.019	0.019
MPWB1K	0.019	−0.013
MPW1K	0.019	−0.014
ωB97	0.020	0.001
OreLYP	0.020	0.017
OLYP	0.021	0.018
PW6B95	0.022	0.007
Hartree−Fock	0.022	−0.007
M11-L	0.023	−0.017
GVWN5	0.024	−0.013
MOHLYP	0.034	0.034
OHLYP	0.036	0.036
HFLYP	0.038	−0.035
SOGGA	0.211	0.196

MUEs and MSEs are shown in Table 13; B3LYP*, revB3LYP, and revTPSSh give the smallest MUEs (0.011 Å) for bond distances. Most of the density functional tested in our article give good results for the geometries, as Table 13 shows 33 density functionals with a mean unsigned error less than or equal to 0.015 Å.

In order to see the correlations between bond distances and energies and dipole moments, we calculated the Pearson

DOI: 10.1021/acs.jctc.5b00083
J. Chem. Theory Comput. 2015, 11, 2968−2983

correlation coefficients for these two correlations. The Pearson correlation coefficient between MUE of bond distances and overall over AUE in Table 11 is 0.15, and that between MUE of bond distances and MUE of dipole moment in Table 12 is −0.13. Note that we do not include the Hartree−Fock method in the Pearson correlation calculations. Therefore, the accuracies of the geometries of tested main-group molecules have very small correlation with their energies and dipole moments. This is consistent with previous observations[62,64] that were made on the basis of less systematic data.

We also calculated the MUEs of bond distances for each molecule against 54 methods. As we can see from Table 10, HF, BeF, and LiF have the smallest MUEs for bond distances (0.006, 0.007, and 0.008 Å, respectively). In contrast, BeO, the OH bond in KOH, and NaO have the largest MUEs for bond distances, with mean magnitudes of their errors four to eight times larger (0.047, 0.044, and 0.029 Å, respectively). BeO is very difficult for both bond distance and bond energy.

4. CONCLUSIONS

We calculated the bond dissociation energies of 15 main-group molecules, 14 of which contain group-1 and group-2 metal atoms, by employing 54 methods, in particular, the Hartree−Fock method and 53 exchange-correlation functionals for Kohn−Sham density functional theory. The T_1, TAE, B_1, and M diagnostics are used to classify these molecules into eight single-reference systems and seven multireference systems. Furthermore, we decomposed the bond dissociation energy into four components to better understand the sources of the errors in the bond dissociation energies. We calculated ionization potential, electron affinity, atomic excitation energy, interaction energy between two prepared valence states, and dipole moment by using all 54 methods.

In order to predict the most accurate bond dissociation energies − on average − with a minimum amount of cancellation of errors, the method should predict the smallest average unsigned error of all of the components that contribute to the energy change upon forming a bond. Whereas M08-HX, ωB97X-D, TPSS, PW6B95-D3(BJ), OreLYP, PW6B95-D3(0), and PW6B95 give the smallest mean unsigned errors for bond dissociation energy, PW6B95-D3(BJ), revTPSS, TPSS, PW6B95-D3(0), PW6B95, M08-HX, PW6B95-D3(0), M05-2X, and B97-1 give the smallest values for average unsigned error of all energetic data of the 15 diatomic molecules.

The PW6B95 functional predicts these main-group molecules very well. The new GAM functional is the best gradient approximation for these main-group molecules, and it is also the best functional for seven multireference systems. The best meta-GGA for these 15 main-group molecules is revTPSS, and it is also the best meta-GGA for eight single-reference systems. The best three functionals in predicting dipole moment are MPWLYP1M, PBE, and O3LYP. Multireference molecules are harder to predict than single-reference molecules because they have a larger mean unsigned error over all functionals. The hardest molecule for energetic predictions is LiO^-, which gives an overall MUE of 9.5 kcal/mol. This study shows the multireference character of main-group diatomic molecules and importance of getting the correct components for each molecule so as to get the correct bond dissociation energy with minimal cancellation of errors. These bond dissociation energies and their components can be used for exchange-correlation functional development. A good functional should predict all five components correctly; otherwise, the small errors may come from cancellation of error. The only functional tested in our article that is able to predict all five components correctly is M06-2X. The MUEs of the bond distances tested in our article have a very small correlation with the MUEs of the dipole moments and the AUEs of overall energies. The best functionals for bond distance are B3LYP*, revB3LYP, and revTPSSh with an error of 0.011 Å. Over a half of the functionals tested in the article give an error no larger than 0.015 Å for the bond distances.

A number of the findings of this study were unexpected. For example, the errors for bond energies involving main-group metals are usually larger than typical errors for bonds between main-group nonmetals. For other examples, some functionals with high percentages of Hartree−Fock exchange do well for multireference systems, and the ability to predict electron affinities of ligands correlates well with the ability to predict accurate metal−ligand bond energies. If we compare Tables 11 and 13 together, then we find that there are some functionals that give small errors for both energy and geometry. For example, B97-1, B97-3, MPW1B95, M05, M05-2X, M06, M06-2X, M08-HX, M08-SO, N12-SX, O3LYP, TPSS, GAM, and τ-HCTHhyb give an MUE for bond distance no larger than 0.015 Å and an overall AUE for energetic quantitates no larger than 5.20 kcal/mol. Of these functionals, Table 12 shows that the following functionals also give a mean unsigned error in dipole moments of 0.85 D or less: B97-1, B97-3, MPW1B95, M05, M06, M06-2X, M08-SO, N12-SX, O3LYP, TPSS, GAM, and τ-HCTHhyb. As we and others attempt to develop improved density functionals for systems containing metal atoms, the data presented here, which gives a snapshot of the current status, provides a standard against which one can measure whether success is being achieved; additionally, this data provides a challenge in that we should try to reduce the errors.

■ ASSOCIATED CONTENT

Supporting Information

Additional information on the PW6B95, PW6B95-D3(0), and PW6B95-D3(BJ) calculations. The Supporting Information is available free of charge on the ACS Publications website at DOI: 10.1021/acs.jctc.5b00083.

■ AUTHOR INFORMATION

Corresponding Author

*E-mail: truhlar@umn.edu.

Funding

This work was supported in part by by the U.S. Department of Energy, Office of Basic Energy Sciences, Division of Chemical Sciences, under award DE-SC0012702 to the Inorganometallic Catalyst Design Center.

Notes

The authors declare no competing financial interest.

■ REFERENCES

(1) Yu, H.; Truhlar, D. G. *J. Chem. Theory Comput.* **2014**, *10*, 2291−2305.
(2) Karton, A.; Rabinovich, E.; Martin, J. M. L.; Ruscic, B. *J. Chem. Phys.* **2006**, *125*, 144108.
(3) Karton, A.; Taylor, P. R.; Martin, J. M. L. *J. Chem. Phys.* **2007**, *127*, 064104.
(4) Raghavachari, K.; Trucks, G. W.; Pople, J. A.; Head-Gordon, M. *Chem. Phys. Lett.* **1989**, *157*, 479−483.
(5) Stephens, P. J.; Devlin, F. J.; Chabalowski, C. F.; Frisch, M. J. *J. Phys. Chem.* **1994**, *98*, 11623−11627.
(6) Møller, C.; Plesset, M. S. *Phys. Rev.* **1934**, *46*, 618−622.

DOI: 10.1021/acs.jctc.5b00083
J. Chem. Theory Comput. 2015, 11, 2968−2983

(7) Martin, H.-G.; Pople, J. A.; Frisch, M. J. *Chem. Phys. Lett.* **1988**, *153*, 503−506.
(8) Karton, A.; Martin, J. M. L. *J. Chem. Phys.* **2010**, *133*, 144102.
(9) Soulé de Bas, B; Dorsett, H. E.; Ford, M. J. *J. Phys. Chem. Solids* **2003**, *64*, 495−505.
(10) Sorensen, T. E.; England, W. B. *Int. J. Quantum Chem.* **2000**, *76*, 259−279.
(11) Irisawa, J.; Iwata, S. *Theor. Chim. Acta.* **1992**, *81*, 223−235.
(12) Nakazato, D. T. I.; De Sá, E. L.; Haiduke, R. L. A. *Int. J. Quantum Chem.* **2010**, *110*, 1729−1737.
(13) Zhao, Y.; Truhlar, D. G. *Theor. Chem. Acc.* **2008**, *120*, 215−241.
(14) Zheng, J.; Xu, X.; Truhlar, D. G. *Theor. Chem. Acc.* **2011**, *128*, 295−305.
(15) Woon, D. E.; Dunning, T. K. J. *J. Chem. Phys.* **1995**, *103*, 4572−4585.
(16) Peterson, K. A.; Dunning, T. H. *J. Chem. Phys.* **2002**, *117*, 10548−10560.
(17) Seeger, R.; Pople, J. A. *J. Chem. Phys.* **1977**, *66*, 3045−3050.
(18) Bauernschmitt, R.; Ahlrichs, R. *J. Chem. Phys.* **1996**, *104*, 9047−9052.
(19) Frisch, M. J.; Trucks, G. W.; Schlegel, H. B.; Scuseria, G. E.; Robb, M. A.; Cheeseman, J. R.; Scalmani, G.; Barone, V.; Mennucci, B.; Petersson, G. A.; Nakatsuji, H.; Caricato, M.; Li, X.; Hratchian, H. P.; Izmaylov, A. F.; Bloino, J.; Zheng, G.; Sonnenberg, J. L.; Hada, M.; Ehara, M.; Toyota, K.; Fukuda, R.; Hasegawa, J.; Ishida, M.; Nakajima, T.; Honda, Y.; Kitao, O.; Nakai, H.; Vreven, T.; Montgomery, J. A., Jr.; Peralta, J. E.; Ogliaro, F.; Bearpark, M.; Heyd, J. J.; Brothers, E.; Kudin, K. N.; Staroverov, V. N.; Kobayashi, R.; Normand, J.; Raghavachari, K.; Rendell, A.; Burant, J. C.; Iyengar, S. S.; Tomasi, J.; Cossi, M.; Rega, N.; Millam, J. M.; Klene, M.; Knox, J. E.; Cross, J. B.; Bakken, V.; Adamo, C.; Jaramillo, J.; Gomperts, R.; Stratmann, R. E.; Yazyev, O.; Austin, A. J.; Cammi, R.; Pomelli, C.; Ochterski, J. W.; Martin, R. L.; Morokuma, K.; Zakrzewski, V. G.; Voth, G. A.; Salvador, P.; Dannenberg, J. J.; Dapprich, S.; Daniels, A. D.; Farkas, O.; Foresman, J. B.; Ortiz, J. V.; Cioslowski, J.; Fox, D. J. *Gaussian 09*, revision C.01; Gaussian, Inc.: Wallingford, CT, 2009.
(20) Roos, B. O.; Taylor, P. R.; Siegbahn, P. E. M. *Chem. Phys.* **1980**, *48*, 157−173.
(21) Tishchenko, O.; Zheng, J.; Truhlar, D. G. *J. Chem. Theory. Comput.* **2008**, *4*, 1208−1219.
(22) Helgaker, T.; Jorgensen, P.; Olsen, J. *Modern Electronic Structure Theory*; Wiley: Chichester, 2000; p 188.
(23) Valiev, M.; Bylaska, E. J.; Govind, N.; Kowalski, K.; Straatsma, T. P.; van Dam, H. J. J.; Wang, D.; Nieplocha, J.; Apra, E.; Windus, T. L.; de Jong, W. A. *Comput. Phys. Commun.* **2010**, *181*, 1477−1489.
(24) Lee, T. J.; Taylor, P. R. *Int. J. Quantum Chem., Symp.* **1989**, *23*, 199−207.
(25) Schultz, N. E.; Zhao, Y.; Truhlar, D. G. *J. Phys. Chem. A* **2005**, *109*, 11127−11143.
(26) Zhao, Y.; Tishchenko, O.; Gour, J. R.; Li, W.; Lutz, J. J.; Piecuch, P.; Truhlar, D. G. *J. Phys. Chem. A* **2009**, *113*, 5786−5799.
(27) Werner, H.-J.; Knowles, P. J.; Manby, F. R.; Schütz, M.; Celani, P.; Knizia, G.; Korona, T.; Lindh, R.; Mitrushenkov, A.; Rauhut, G.; Adler, T. B.; Amos, R. D.; Bernhardsson, A.; Berning, A.; Cooper, D. L.; Deegan, M. J. O.; Dobbyn, A. J.; Eckert, F.; Goll, E.; Hampel, C.; Hesselmann, A.; Hetzer, G.; Hrenar, T.; Jansen, G.; Köppl, C.; Liu, Y.; Lloyd, A. W.; Mata, R. A.; May, A. J.; McNicholas, S. J.; Meyer, W.; Mura, M. E.; Nicklaß, A.; Palmieri, P.; Pflüger, K.; Pitzer, R.; Reiher, M.; Shiozaki, T.; Stoll, H.; Stone, A. J.; Tarroni, R.; Thorsteinsson, T.; Wang, M.; Wolf, A. *Molpro*, version 2010.1; University of Birmingham: Birmingham, UK, 2010.
(28) Čížek, J. In *Advances in Chemical Physics*; Hariharan, P. C., Ed.; Wiley Interscience: New York, 1969; Vol. *14*, p 35ff.
(29) Purvis, G. D., III; Bartlett, R. J. *J. Chem. Phys.* **1982**, *76*, 1910−1918.
(30) Scuseria, G. E.; Janssen, C. L.; Schaefer, H. F., III *J. Chem. Phys.* **1988**, *89*, 7382−7387.
(31) Scuseria, G. E.; Schaefer, H. F., III *J. Chem. Phys.* **1989**, *90*, 3700−3703.
(32) Becke, A. D. *Phys. Rev. A* **1988**, *38*, 3098−3100.
(33) Lee, C.; Yang, W.; Parr, R. G. *Phys. Rev. B* **1988**, *37*, 785−789.
(34) Adamo, C.; Barone, V. *Chem. Phys. Lett.* **1997**, *274*, 242−250.
(35) Marenich, A. V.; Jerome, S. V.; Cramer, C. J.; Truhlar, D. G. *J. Chem. Theory Comput.* **2012**, *8*, 527−541.
(36) Goerikg, L.; Grimme, S. *Phys. Chem. Chem. Phys.* **2011**, *13*, 6670−6688.
(37) Yu, S. H.; Zhang, W.; Verma, P.; He, X. *Phys. Chem. Chem. Phys.* **2015**, *17*, 12146−12160.
(38) Lu, L.; Hu, H.; Huo, H.; Wang, B. *Comput. Theor. Chem.* **2013**, *1051*, 64−71.
(39) Douglas, M.; Kroll, N. M. *Ann. Phys* **1974**, *82*, 89−155.
(40) Hess, B. A. *Phys. Rev. A* **1985**, *32*, 756−763.
(41) Hess, B. A. *Phys. Rev. A* **1986**, *33*, 3742−3748.
(42) Moore, C. E. *Atomic Energy Levels*; National Bureau of Standards, U. S. Government Printing Office: Washington, DC, 1949−1958; Vol. *I*.
(43) Roos, B. O.; Taylor, B. R.; Siegbahn, P. E. M. *Chem. Phys.* **1980**, *48*, 157−173.
(44) Holthausen, M. C.; Mohr, M.; Koch, W. *Chem. Phys. Lett.* **1995**, *240*, 245−252.
(45) Luo, Y.-R.; Cheng, J.-P. In *Handbook of Chemistry and Physics*, 95th ed.; Lide, D. R., Ed.; CRC Press: Boca Raton, FL, 2015; Section 9, pp 65−69.
(46) BauSchlicher, C. W., Jr; Lengsfield, B. H., III; Liu, B. *J. Chem. Phys.* **1982**, *77*, 4084−4087.
(47) *Handbook of Chemistry and Physics*, 95th ed.; Lide, D. R., Ed.; CRC Press: Boca Raton, FL, 2015; Section 10, pp 197−199.
(48) Miller, T. M. In *Handbook of Chemistry and Physics*, 95th ed.; Lide, D. R., Ed.; CRC Press: Boca Raton, FL, 2015; Section 10, pp. 147−149.
(49) *Gas phase ion energetics data*; National Institute of Standards and Technology: Gaithersburg, MD. http://webbook.nist.gov/cgi/cbook.cgi?ID=C3352576&Mask=20.
(50) Lide, D. R. In *Handbook of Chemistry and Physics*, 95th ed.; Lide, D. R., Ed.; CRC Press: Boca Raton, FL, 2015; Section 9, pp 102−107.
(51) Lide, D. R. In *Handbook of Chemistry and Physics*, 95th ed.; Lide, D. R., Ed.; CRC Press: Boca Raton, FL, 2015; Section 9, pp 51−59.
(52) *Experimental Bond Length Data*; National Institute of Standards and Technology: Gaithersburg, MD/ http://cccbdb.nist.gov/expbondlengths1.asp.
(53) Ghalila, H.; Lahmar, S.; Lakhdar, Z. B.; Hochlaf, M. *J. Phys. B: At., Mol. Opt. Phys.* **2008**, *41*, 205101.
(54) Yoshimine, M. *J. Phys. Soc. Jpn.* **1968**, *25*, 1100−1119.
(55) Kohn, W.; Sham, L. J. *Phys. Rev.* **1965**, *140*, A1133−A1138.
(56) (a) Gáspár, R. *Acta Phys. Hung.* **1954**, *3*, 263−286. (b) Gáspár, R. *Acta Phys. Hung.* **1974**, *35*, 213−218.
(57) Vosko, S. H.; Wilk, L.; Nusair, M. *Can. J. Phys.* **1980**, *58*, 1200−1211.
(58) Becke, A. D. *J. Chem. Phys.* **1996**, *104*, 1040−1046.
(59) Handy, N. C.; Cohen, A. J. *Mol. Phys.* **2001**, *99*, 403−412.
(60) Thakkar, A. J.; McCarthy, S. P. *J. Chem. Phys.* **2009**, *131*, 134109.
(61) Perdew, J. P.; Burke, K.; Ernzerhof, M. *Phys. Rev. Lett.* **1996**, *77*, 3865−3868.
(62) Zhao, Y.; Truhlar, D. G. *J. Chem. Phys.* **2008**, *128*, 184109.
(63) Peverati, R.; Zhao, Y.; Truhlar, D. G. *J. Phys. Chem. Lett.* **2011**, *2*, 1991−1997.
(64) Peverati, R.; Truhlar, D. G. *J. Chem. Theory Comput.* **2012**, *8*, 2310−2319.
(65) Zhao, Y.; Truhlar, D. G. *J. Chem. Phys.* **2006**, *125*, 194101.
(66) Peverati, R.; Truhlar, D. G. *J. Phys. Chem. Lett.* **2011**, *3*, 117−124.
(67) Perdew, J. P.; Ruzsinszky, A.; Csonka, G. I.; Constantin, L. A.; Sun, J. *Phys. Rev. Lett.* **2009**, *103*, 026403.
(68) Tao, J. M.; Perdew, J. P.; Staroverov, V. N; Scuseria, G. E. *Phys. Rev. Lett.* **2003**, *91*, 146401.
(69) Peverati, R.; Truhlar, D. G. *Phys. Chem. Chem. Phys.* **2012**, *14*, 13171−13174.
(70) Reiher, M.; Salomon, O.; Hess, B. A. *Theor. Chem. Acc.* **2001**, *107*, 48−55.
(71) Hamprecht, F. A.; Cohen, A. J.; Tozer, D. J.; Handy, N. C. *J. Chem. Phys.* **1988**, *109*, 6264−6271.

DOI: 10.1021/acs.jctc.5b00083
J. Chem. Theory Comput. 2015, 11, 2968−2983

(72) Keal, T. W.; Tozer, D. J. *J. Chem. Phys.* **2005**, *123*, 121103.
(73) Valentin, C. D.; Pacchioni, G.; Bredow, T.; Dominguez-Ariza, D.; Illas, F. *J. Chem. Phys.* **2002**, *117*, 2299−2306.
(74) Lynch, B. J.; Fast, P. L.; Harris, M.; Truhlar, D. G. *J. Phys. Chem. A* **2000**, *104*, 4811−4815.
(75) Hoe, W.-M.; Cohen, A. J.; Handy, N. C. *Chem. Phys. Lett.* **2001**, *341*, 319−328.
(76) Adamo, C.; Barone, V. *J. Chem. Phys.* **1999**, *110*, 6158−6170.
(77) Peverati, R.; Truhlar, D. G. *J. Chem. Phys.* **2011**, *135*, 191102.
(78) Zhao, Y.; Lynch, B. J.; Truhlar, D. G. *J. Phys. Chem. A* **2004**, *108*, 2715−2719.
(79) Zhao, Y.; Schultz, N. E.; Truhlar, D. G. *J. Chem. Phys.* **2005**, *123*, 161103.
(80) Zhao, Y.; Schultz, N. E.; Truhlar, D. G. *J. Chem. Theory Comput.* **2006**, *2*, 364−382.
(81) Zhao, Y.; Truhlar, D. G. *J. Chem. Theory Comput.* **2008**, *4*, 1849−1868.
(82) Zhao, Y.; Truhlar, D. G. *J. Phys. Chem. A* **2004**, *108*, 6908−6918.
(83) Zhao, Y.; Truhlar, D. G. *J. Phys. Chem. A* **2005**, *109*, 5656−5667.
(84) Csonka, G. I.; Perdew, J. P.; Ruzsinszky, A. *J. Chem. Theory Comput.* **2010**, *6*, 3688−3703.
(85) Staroverov, V. N.; Scuseria, G. E.; Tao, J.; Perdew, J. P. *J. Chem. Phys.* **2003**, *119*, 12129−12137.
(86) Boese, A. D.; Handy, N. C. *J. Chem. Phys.* **2002**, *116*, 9559−9569.
(87) Yanai, T.; Tew, D.; Handy, N. *Chem. Phys. Lett.* **2004**, *393*, 51−57.
(88) Heyd, J.; Scuseria, G. E.; Ernzerhof, M. *J. Chem. Phys.* **2003**, *118*, 8027−8215.
(89) Henderson, T. M.; Izmaylov, A. F.; Scalmani, G.; Scuseria, G. E. *J. Chem. Phys.* **2009**, *131*, 044108.
(90) Chai, J.-D.; Head-Gordon, M. *J. Chem. Phys.* **2008**, *128*, 084106.
(91) Peverati, R.; Truhlar, D. G. *Phys. Chem. Chem. Phys.* **2012**, *14*, 16187−16191.
(92) Peverati, R.; Truhlar, D. G. *J. Phys. Chem. Lett.* **2011**, *2*, 2810−2817.
(93) Chai, J.-D.; Head-Gordon, M. *Phys. Chem. Chem. Phys.* **2008**, *10*, 6615−6620.
(94) Becke, A. D.; Johnson, E. R. *J. Chem. Phys.* **2005**, *122*, 154101.
(95) Johnson, E. R.; Becke, A. D. *J. Chem. Phys.* **2005**, *123*, 024101.
(96) Johnson, E. R.; Becke, A. D. *J. Chem. Phys.* **2006**, *124*, 174104.

DOI: 10.1021/acs.jctc.5b00083
J. Chem. Theory Comput. 2015, 11, 2968−2983